Characterization of Starburst Dendrimers by Electron Paramagnetic Resonance. 2. Positively Charged Nitroxide Radicals of Variable Chain Length Used as Spin Probes

M. Francesca Ottaviani,*,† Eleonora Cossu,† Nicholas J. Turro,‡ and Donald A. Tomalia§

Contribution from the Department of Chemistry, University of Florence, 50121 Firenze, Italy, Department of Chemistry, Columbia University, New York, New York 10027, and Michigan Molecular Institute, Midland, Michigan 48640

Received December 5, 1994®

Abstract: Electron paramagnetic resonance (EPR) spectroscopy has been used to investigate the structure and binding ability of a novel class of anionic macromolecules: half-generation poly(amidoamine) starburst dendrimers (*n*.5-SBDs), which differ systematically in size (generation), and which are terminated by sodium carboxylated surfaces. The half-generations in the range 1.5–7.5 have been investigated. To some extent *n*.5-SBDs mimic both anionic micelles, in their shape and external surface, and biomacromolecules, such as proteins and enzymes, in their internal structure. Positively charged nitroxide radicals attached to carbon chains of different lengths were used to probe hydrophilic and hydrophobic binding sites of the SBD structure. Mobility and polarity parameters were evaluated by means of a computer-aided analysis of the EPR spectra of the interacting radicals. The study of these parameters as a function of pH demonstrated the role of electrostatic interactions in promoting binding at the external SBD/water interface. Such interactions are found to be weaker than those occurring with anionic micelles, due to the greater hydrophilic character of the internal SBD structure. Analysis of the EPR parameters as a function of radical chain length, generation, and carboxylate concentration provided evidence of both hydrophilic and hydrophobic interactions between the probe radicals and *n*.5-SBDs. The results are consistent with the hypothesis that the radical chain may enter the SBD internal structure and interact with hydrophobic sites. Analysis of EPR spectra at different temperatures provided the activation energies for the rotational motion of the interacting probe.

Introduction

The novel class of macromolecules designated as starburst dendrimers (SBDs) are mainly characterized by high symmetry and low dispersity, since the monomers are covalently attached in radially branched layers, termed generations, to a central core.[1] These polymers belong to the family of dendritic macromolecules which have attracted considerable attention in recent years.[2] On the basis of molecular simulations,[3] the morphology of SBDs has been computed to possess open structures and asymmetric disklike shapes for the low generations, termed earlier generations ($G = 2-3$), and densely packed structures and spherical shapes for the high generations, termed later generations ($G \geq 4$). Photophysical studies have provided support to the validity of this computation.[4] We focused our interest on the poly(amidoamine) (PAMAM) family of SBDs which is obtained by the grafting of amidoamine units to a central nitrogen core.[1a] This family of SBDs is of particular interest because the internal poly(amidoamine) structure mimics well the structure of biomacromolecules, such as proteins and enzymes, but also manifests a very useful difference of a much higher stability with respect to external agents. The progressive growth of generations creates organized arrangements of various sizes, which are shown schematically in Figure 1. This figure displays a two-dimensional projection of the so-called half-generation PAMAM SBDs, which are characterized by carboxylate groups (sodium gegenions) at the external surface. Henceforth in this paper, this family of SBDs is designated *n*.5-SBD. Due to their shape and interfacial properties, these *n*.5-SBDs resemble anionic micelles.[1a,c,j] However, the dendritic macromolecules described in refs 5–9 much better represent unimolecular micelles since their interior core is more hydrophobic, if compared to *n*.5-SBDs. An advantage of the *n*.5-SBDs is mainly in that they are good models for both biomacromolecules and anionic micelles. Also, the electron-

* Address correspondence to Dr. M. Francesca Ottaviani, Dipartimento di Chimica, Via G. Capponi 9, 50121 Firenze, Italy.

† University of Florence.

‡ Columbia University.

§ Michigan Molecular Institute.

® Abstract published in *Advance ACS Abstracts*, March 15, 1995.

(1) (a) Tomalia, D. A.; Baker, H.; Dewald, J.; Hall, M.; Kallos, G.; Martin, S.; Roeck, J.; Smith, P. *Polym. J. (Tokyo)* **1985**, *17*, 117. (b) *Macromolecules* **1986**, *19*, 2466. (c) Tomalia, D. A.; Berry, V.; Hall, M.; Hedstrand, D. M. *Macromolecules* **1987**, *20*, 1164. (d) Tomalia, D. A.; Hall, M.; Hedstrand, D. M. *J. Am. Chem. Soc.* **1987**, *109*, 1601. (e) Padias, A. B.; Hall, H. K.; Tomalia, D. A.; McConnell, J. R. *J. Org. Chem.* **1987**, *52*, 5305. (f) Wilson, L. R.; Tomalia, D. A. *Polym. Prepr. (Am. Chem. Soc., Div. Polym. Chem.)* **1989**, *30*, 115. (g) Padias, A. B.; Hall, H. K.; Tomalia, D. A. *Polym. Prepr. (Am. Chem. Soc. Div. Polym. Chem.)* **1989**, *30*, 119. (h) Meltzer, A. D.; Tirell, D. A.; Jones, A. A.; Inglefield, P. T.; Downing, D. M.; Tomalia, D. A. *Polym. Prepr. (Am. Chem. Soc., Div. Polym. Chem.)* **1989**, *30*, 121. (i) Tomalia, D. A.; Naylor, A. M.; Goddard, W. A., III. *Angew. Chem., Int. Ed. Engl.* **1990**, *29*, 138. (j) Tomalia, D. A.; Dewald, J. R. U.S. Patent 4 507 466, 1985; U.S. Patent 4 558 120, 1985; U.S. Patent 4 568 737, 1986; U.S. Patent 4 587 329, 1986; U.S. Patent 4 631 337, 1986; U.S. Patent 4 694 064, 1986; U.S. Patent 4 857 599, 1989.

(2) *Advances in Dendritic Macromolecules*; Newkome, G. R., Ed.; JAI Press: Greenwich, CT, 1993.

(3) Naylor, A. M.; Goddard, W. A., III; Kiefer, G. E.; Tomalia, D. A. *J. Am. Chem. Soc* **1989**, *111*, 2341.

(4) Moreno-Bondi, M.; Orellana, G.; Turro, N. J.; Tomalia, D. A. *Macromolecules* **1990**, *23*, 910.

(5) Newkome, G. R.; Moorefield, C. N.; Baker, G. R.; Johnson, A. L.; Behera, R. K. *Angew. Chem., Int. Ed. Engl.* **1991**, *30*, 1176.

(6) Newkome, G. R ; Moorefield, C. N.; Baker, G. R.; Saunders, M. J.; Grossman, S. H. *Angew. Chem., Int. Ed. Engl.* **1991**, *30*, 1178.

(7) Kim, Y. H.; Webster, O. W. *J. Am. Chem. Soc.* **1990**, *112*, 4592.

(8) Hawker, C. J.; Wooley, K. L.; Fréchet, J. M. J. *J. Chem. Soc., Perkin Trans. 1* **1993**, 1287.

(9) Newkome, G. R.; Young, J. K.; Baker, G. R.; Potter, R. L.; Audoly, L; Cooper, D.; Weis, C. D. *Macromolecules* **1993**, *26*, 2394.

0002-7863/95/1517-4387$09.00/0

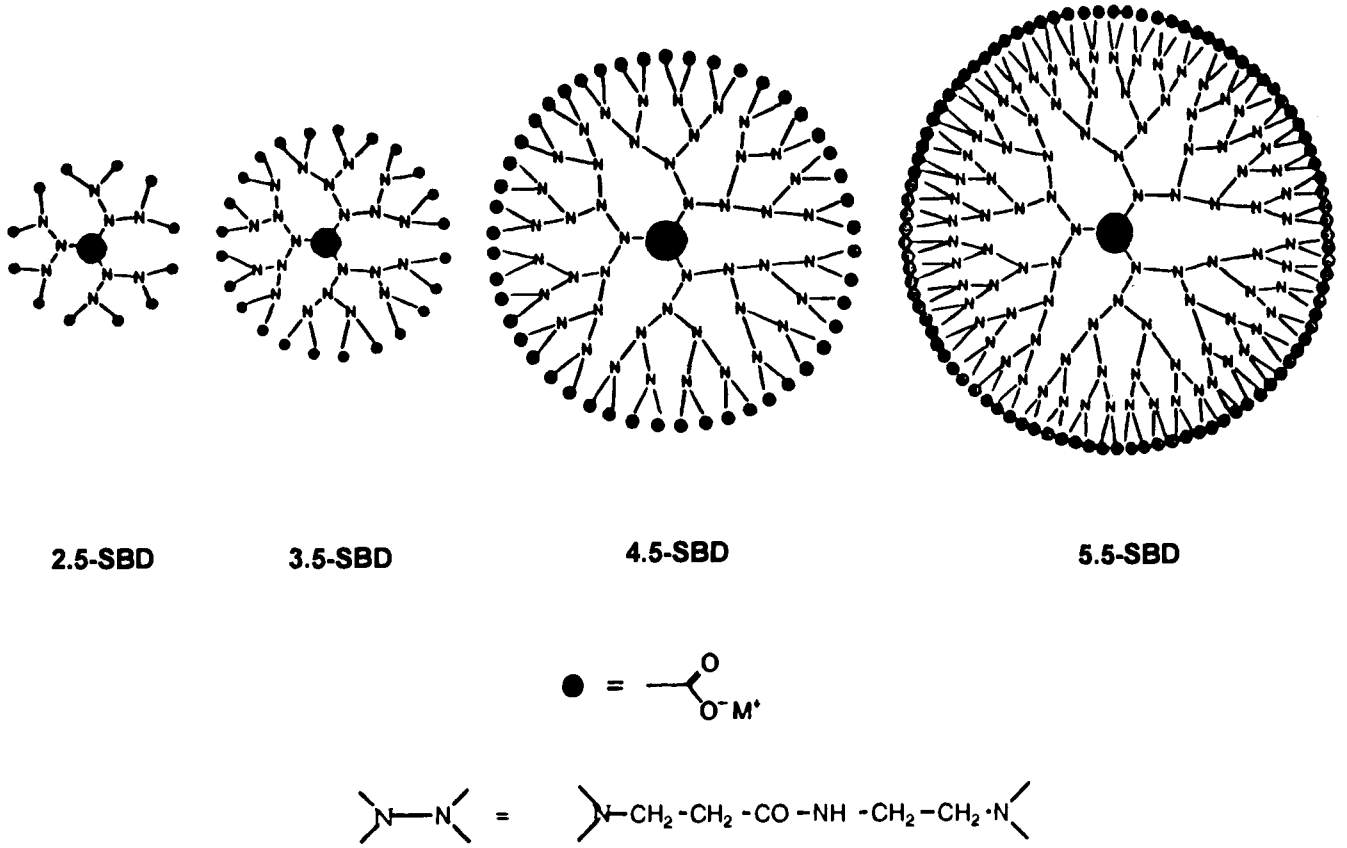

Figure 1. Two-dimensional projection of half-generation PAMAM starburst dendrimers with carboxylate groups at the external surface, termed *n*.5-SBDs. In this manuscript and in future manuscripts, the original nomenclature[1a] for labeling the starburst generation will be adopted. The reason for this change is that the original nomenclature possesses a direct intuitive connection with dendrimer structure.

transfer quenching of photoexcited $Ru(Phen)_3^{2+}$ by methylviologen has provided further evidence of the similarities between *n*.5-SBDs and anionic micelles.[10]

Using spin-label and spin-probe techniques, electron paramagnetic resonance (EPR) has proven to be a very useful tool in investigating the properties of polymeric and macromolecular systems which are of biochemical or industrial relevance.[11,12] In particular, nitroxide spin-labels and spin-probes have been successfully used in obtaining information on micellar solutions.[13-19] For instance, long chain nitroxides have been shown to be very profitable in studying the micellization process and the properties of micellar solutions, since the hydrophobic chain of these nitroxides may be inserted in the hydrophobic core of the micelles. In the case of *n*.5 SBDs, the internal structure is mainly hydrophilic in nature (amido functions), but in line with similar biomacromolecular structures, it may offer both hydrophilic and hydrophobic interacting sites (such as $=NCH_2CH_2CO-$) to guest molecules and ions which are able to penetrate the external, charged double layer.

Very recently Cu(II) ions have been used to study the interacting abilities of the various internal and external ligand sites of *n*.5 SBDs.[20] Various Cu(II) complexes, corresponding to differing binding sites, are formed as a function of generation and pH. All the results confirm the similarities between the internal SBD structure and the structure of proteins and enzymes. However, Cu(II) ions, due to their powerful interacting ability, are indeed both strongly perturbative and selective in their interactions. The use of radicals as probes is usually very advantageous in obtaining information on environmental properties and is expected to be less perturbative. Therefore, in the present study, nitroxide radicals were used to investigate the structural properties of *n*.5-SBDs and their interactions with the radical molecules. A positively charged nitroxide was chosen to bind electrostatically with the negatively charged *n*.5-SBD surface. Furthermore, attached carbon chains of different lengths permitted investigation of interactions occurring at the more hydrophobic interacting sites of *n*.5-SBDs. The interactions of a positively charged surfactant, namely, dodecyltrimethylammonium bromide (DTAB), with the *n*.5-SBDs have also been analyzed by Caminati *et al.*,[21] by means of the fluorescence probe method.

In summary, the present investigation addresses the following topics: (1) The interacting ability of the negatively charged

(10) Gopidas, K. R.; Leheny, A. R.; Caminati, G.; Turro, N. J.; Tomalia, D. A. *J. Am. Chem .Soc.* **1991**, *113*, 7335.
(11) *Spin Labeling. Theory and Applications*; Berliner, L. J., Ed.; Academic Press: New York, 1976; Vol. 1; 1979; Vol. 2.
(12) *Biological Magnetic Resonance. Spin Labeling. Theory and Applications*; Berliner, L. J., Reuben, J., Eds.; Plenum Press: New York, 1989; Vol. 8.
(13) Taupin, C; Dvolaitoky, M. In *Surfactant Solutions. New Methods of Investigation*; Zana, R., Ed.; Surfactant Science Series; Marcel Dekker: New York, 1987; Vol. 22, p 359.
(14) Hearing, G.; Luisi, P. L.; Hauser, H. *J. Phys. Chem.* **1983**, *92*, 3574.
(15) Yoshioka, H., Kazama, S. *J. Colloid Interface Sci.* **1983**, *95*, 240.
(16) Barelli, A.; Heicke, H. F. *Langmuir* **1986**, *2*, 780.
(17) (a) Ottaviani, M. F.; Baglioni, P.; Martini, G. *J. Phys. Chem.* **1983**, *87*, 3146. (b) Baglioni, P.; Ferroni, E.; Martini, G.; Ottaviani, M. F. *J. Phys. Chem.* **1984**, *88*, 5187. (c) Baglioni, P.; Ottaviani, M. F.; Martini, G. *J. Phys. Chem.* **1986**, *90*, 5878.
(18) Bratt, J. P.; Kevan, L. *J. Phys. Chem.* **1992**, *96*, 6849; **1993**, *97*, 6849.
(19) (a) Martini, G.; Ottaviani, M. F.; Ristori, S.; Lenti, D.; Sanguineti, A. *Colloids Surf.* **1990**, *45*, 177. (b) Bonosi, F.; Gabrielli, G.; Margheri, E.; Martini, G. *Langmuir* **1990**, *6*, 1769. (c) Ristori, S.; Ottaviani, M. F.; Lenti, D.; Martini, G. *Langmuir* **1991**, *7*, 1958. (d) Ristori, S.; Martini, G *Langmuir* **1992**, *8*, 1937. (e) Martini, G.; Ottaviani, M. F.; Ristori, S. *Croat. Chim. Acta* **1992**, *65*, 471. (f) Ottaviani, M. F.; Ghatlia, N. D.; Turro, N. J. *J. Phys. Chem.* **1992**, *96*, 6075.
(20) Ottaviani, M. F.; Bossmann, S.; Turro, N. J.; Tomalia, D. A. *J. Am. Chem. Soc.* **1994**, *116*, 661.
(21) Caminati, G.; Turro, N. J.; Tomalia, D. A. *J. Am. Chem. Soc.* **1990**, *112*, 8515.

external surface of the *n*.5-SBDs toward positively charged probes whose size and hydrophobicity inhibits deep penetration of the internal hydrophilic structure of the SBD. In this respect, it is of interest to investigate the influence of varying extent of ionization of the surface (as a function of pH) and the influence of the variation of charge density (as a function of generation) on the binding ability of cations to the SBD surface. The results are compared with those obtained with micellar solutions of negatively charged surfactants in the presence of the same radicals. (2) The occurrence of both hydrophobic and hydrophilic interactions with binding sites in the presence of positively charged nitroxide radicals with carbon chains of different lengths. The concentration of the radicals was maintained as low as possible to avoid self-aggregation of the surfactant probes. (3) The effect of temperature variations and the determination of activation energy for rotational motion to obtain further information on the interactions of the nitroxides with interacting sites at the SBD external surface and internal core.

The EPR probes employed were 4-ammonio-2,2,6,6-tetramethylpiperidine-*N*-oxyl iodide derivatives, mainly 4-(*N*,*N*,*N*-trimethylammonio)- (=CAT1), 4-(*N*,*N*-dimethyl-*N*-octylammonio)- (=CAT8), 4-(*N*,*N*-dimethyl-*N*-decylammonio)- (=CAT10), 4-(*N*,*N*-dimethyl-*N*-dodecylammonio)- (=CAT12), 4-(*N*,*N*-dimethyl-*N*-hexadecylammonio)- (=CAT16):

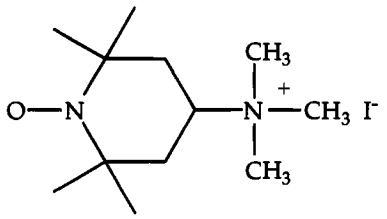

= CAT1

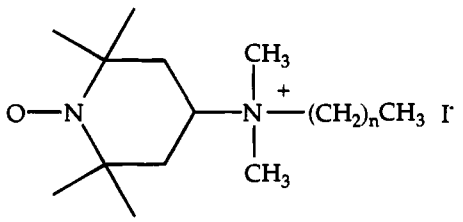

= CATn

The reported experiments were performed in aqueous solutions of *n*.5-SBDs, in the range of generations 1.5–7.5.

Evaluation of Mobility and Polarity Parameters

EPR analysis has been carried out by the evaluation of the correlation times for motion and the hyperfine coupling constants of the radicals in the presence of *n*.5-SBDs. For evaluation of the correlation times for motion, the EPR spectra have been computed by means of the well-established procedure developed by Schneider and Freed.[22] A Brownian rotational diffusion motion was assumed to modulate the magnetic parameters. Therefore, the correlation time, τ_c, is the time characteristic for the rotational diffusion and is related to the rotational diffusion coefficient, D, by the relationship $\tau_c = 1/6D$. The program employed solves the stochastic Liouville equation (the time dependence of the spin density operator) in which the spin Hamiltonian includes not only the Zeeman (electron spin–magnetic field) and hyperfine (electron spin–nuclear spin) interactions, but also contains a restoring potential for oriented samples and the Heisenberg exchange coupling (isotropic electron spin–electron spin interaction). Therefore, the main input parameters to be used in the calculation of the spectra described in this work are (i) the principal components of the **g** and $\mathbf{A}_N$ tensors for the Zeeman and hyperfine coupling, respectively, (ii) the parallel and perpendicular components of the rotational diffusion tensor **D**, since an axial symmetry is assumed, (iii) the Heisenberg spin exchange frequency, ω_{ex}, and (iv) the intrinsic line width $1/T_{2,0}$, which accounts for inhomogeneous, dipolar broadening.

Most of the spectra at room temperature under various experimental conditions are characteristic of the so-called fast motion conditions ($\tau_c < 2-3 \times 10^{-9}$ s), in which the usual three nitrogen hyperfine lines of nitroxides are modified in their relative widths for variations of the environmental microviscosity. In this case, the widths of each hyperfine component, $\Delta H(m_N)$, may be calculated by means of the simplified formula[23,24]

$$\Delta H(m_N) = A + Bm_N + Cm_N^2 \qquad (1)$$

where A contains contributions arising from the anisotropies of the **g** and **A** tensors and terms which are not motional, such as spin rotational relaxation, and unresolved hyperfine structure. The B and C terms also contain the anisotropic components of the **g** and **A** tensors and the spin densities in terms of two correlation times for motion, τ_B and τ_C, respectively. The condition $\tau_B \neq \tau_C$ is assumed to imply anisotropic Brownian motion. Therefore, the values of τ_B and τ_C can be easily calculated, assuming that the line widths of the three m_N manifolds are known.

For the variations of the correlation time for motion in a series of measurements on the same radical with the same experimental conditions, the following simplified formulas have been used to evaluate τ_B and τ_C:

$$\tau_B = B^*\Delta H_0[(h_0/h_1)^{1/2} - (h_0/h_{-1})^{1/2}]$$

$$\tau_C = C^*\Delta H_0[(h_0/h_1)^{1/2} + (h_0/h_{-1})^{1/2} - 2] \qquad (2)$$

where h_i are the peak heights. By solving eq 1, τ_B and τ_C were evaluated and substituted in eq 2. The solution of this last equation gave $B^* \approx C^* \approx 4.9 \times 10^{-10}$, which is different from the value $B^* \approx C^* \approx 6.5 \times 10^{-10}$ used for nitroxide radicals in water solution.[19] However, $B^* \approx C^* \approx 4.9 \times 10^{-10}$ also gave correlation times for motion in good agreement with the values obtained by the computational procedure. Where not otherwise specified, the correlation times for motion reported in the plots as a function of concentration, generation, or temperature are obtained from $\tau_c = (\tau_B\tau_C)^{1/2}$. The accuracy in the determination of τ_c is 2%.

The hyperfine coupling constants may be evaluated as $\langle A_N \rangle = (A_{xx} + A_{yy} + A_{zz})/3$. The A_{ii} components were obtained by computing the spectra at room and low temperatures. However, in a series of measurements on the same radical and at the same experimental conditions, the evaluation of $\langle A_N \rangle$ was performed as peak to peak distances in the experimental spectra. The accuracy in the determination of $\langle A_N \rangle$ is ±0.005 G (based on very good reproducibility of the data). As is well known, $\langle A_N \rangle$ is a good parameter to measure the environmental polarity,[25] since the electron spin density at the nitrogen nucleus increases if the NO mojety is surrounded by more polar molecules.

Experimental Section

n.5-SBDs have been synthesized by published methods.[1] Table 1 lists the molecular weights, the diameters (obtained by size exclusion chromatography (SEC)), the number of surface groups, and the

(22) Schneider, D. J.; Freed, J. H. In *Biological Magnetic Resonance. Spin Labeling. Theory and Applications*; Berliner, L. J., Reuben, J., Eds.; Plenum Press: New York, 1989; Vol. 8, p 1.

(23) Kivelson, D. *J. Chem. Phys.* **1960**, *33*, 1094.

(24) Jolicoeur, C.; Friedman, H. L. *Ber. Bunsen-Ges. Phys. Chem.* **1971**, *75*, 248.

(25) Ottaviani, M. F.; Martini, G; Nuti, L. *Magn. Reson. Chem.* **1987**, *25*, 897.

Table 1. Parameters Relevant to the Size and Surface Characteristics of Starburst Dendrimers

generation	MW	diameter[a]	surface grps[b]	sepn[c]
1.5	924	27.9	6	12.4
2.5	2173	36.2	12	12.8
3.5	4671	48.3	24	12.7
4.5	9668	66.1	48	12.6
5.5	19661	87.9	96	11.5
6.5	39648	103.9	192	10.3
7.5	79621	126.8	384	9.8

[a] Diameter in angstroms determined by size exclusion chromatography (SEC) in water. [b] Number of surface groups. [c] Distance in angstroms between surface groups.

calculated distances between the surface groups for the *n*.5-SBDs used in the present work. It was not possible to study generations larger than 7.5, since the water solubility strongly decreased for the high generations and we were unable to achieve the desired high ratios between the number of surface COO^- groups and the radical concentration. Generations from 1.5 to 7.5 were throughly purified from water and the surface COOH groups completely neutralized with NaOH. The surface groups are henceforth termed SBD-COO^- and it is assumed that the gegenion is Na^+. The pH of the *n*.5-SBDs in water is approximately 9 and was measured with a homemade pH meter equipped with a microelectrode permitting the measurement of small volumes (0.2−0.4 mL). Addition of dilute HCl solution was utilized to decrease the pH to 4. Solutions of pH lower than 4 or higher than 9 were not investigated, since the radicals decompose under such conditions. Solutions of the *n*.5-SBDs in millipore bidistilled water were prepared at concentrations between 1×10^{-3} and 0.85 M in SBD-COO^- at constant concentration of radicals. Comparison among different generations under various experimental conditions, as described in the text, were performed at [SBD-COO^-] = 0.32 M. Unless otherwise specified, the concentrations of *n*.5-SBD were always expressed in terms of the concentration of surface SBD−COO^- groups. The solutions were analyzed after at least 24 h of equilibration; further aging of the solutions did not modify the results. CAT1, CAT8, CAT10, CAT12, and CAT16 were purchased from Molecular Probes and were used without any further purification. Solutions of CAT1, CAT8, CAT10, and CAT12 in bidistilled millipore water were prepared at a concentration of 2 mM and diluted as necessary for each sample, whereas CAT16 was directly added to bidistilled millipore water and to *n*.5-SBD solutions at the proper amount for each sample. All the radical solutions were stored in a refrigerator immediately after preparation. The solutions are expected to contain radical monomers, since the concentrations were below the critical micellar concentration (cmc) of the surfactants. Indeed, the cmc reported for CAT12 at 295 K is 7.1 mM.[26] For CAT16 a cmc of 0.25 mM was determined by means of surface tension measurements (results not shown).

The samples of *n*.5-SBDs containing CAT*n* as a monomeric probe are characterized by a minimum ratio between CAT*n* molecules and SBD-COO^- groups of 1:1000. For instance, the 0.32 M solutions of SBD-COO^- contain CAT*n* at a maximum concentration of 0.3 mM. This corresponds to 1 CAT*n* molecule for approximately two and a half 7.5-SBD molecules to achieve a 0.32 M solution of SBD-COO^- (the number of SBD molecules increases as the generation decreases) and should ensure negligible perturbation of the system by the probes. The study of the variation of mobility and polarity parameters as a function of SBD-COO^- concentration was performed at a constant CAT*n* concentration of 0.17 mM.

The EPR spectra were recorded using a Bruker 200D spectrometer operating in the X band, interfaced with Stelar software to a PC-IBM computer for data acquisition and handling. The temperature was controlled with the aid of a Bruker ST 100/700 variable-temperature assembly. Magnetic parameters were measured by field calibration with the diphenylpicrylhydrazyl (DPPH) radical ($g = 2.0036$).

Results and Discussion

Figure 2 displays experimental (full lines) and calculated (dashed lines) EPR spectra of CAT12 (0.16 mM) in water and in a solution containing 16 mM 4.5-SBD (0.76 M in SBD-COO^-). The experimental spectra were recorded at 298 K. The computation of the spectrum of CAT12 in water has been performed, as described above, employing the program of Schneider and Freed[22] with the magnetic parameters reported for the same radical in ref 19c

$$g_{xx} = 2.0088 \qquad A_{xx} = 6.8 \text{ G}$$

$$g_{yy} = 2.0072 \qquad A_{yy} = 8.2 \text{ G}$$

$$g_{zz} = 2.0035 \qquad A_{zz} = 35.7 \text{ G}$$

$$\langle g \rangle = 2.0065 \qquad \langle A_N \rangle = 16.9 \text{ G}$$

and the residual line width $1/T_{2,0} = 0.5$ G. Only the A_{zz} value varies slightly from 35.7 to 35.6 G when the spectrum of CAT12 in 4.5-SBD solution is calculated. Indeed the two spectra have the following main parameters:

solution	$\langle A_N \rangle$ (G)	τ_c (10^{-10} s)	$1/T_{2,0}$ (G)
water	16.74	0.72	0.5
4.5-SBD	16.68	2.35	0.7

where $\langle A_N \rangle$ was determined from the peak to peak distance in the experimental spectra, and τ_c and $1/T_{2,0}$ are input parameters used for computation. The variation of $\langle A_N \rangle$ from water solution to 4.5-SBD solution is probably within the precision of the analysis, thus indicating that the average environmental polarity of the radical group does not change when CAT12 and 4.5-SBD are mixed. This requires that the radical experiences a very polar (hydrophilic) environment when bound. On the contrary, the mobility of the probe clearly increases upon the addition of 4.5-SBD to the solution. The increase in τ_c is indicative of "interactions" (i.e., binding) between the probe and the SBD molecules. The scope of the following analysis is to clarify the type and mechanism of these interactions, by analyzing the EPR spectra under various experimental conditions.

1. CAT*n* with Varying Chain Lengths, with and without 4.5-SBD. Figure 3 shows a plot of the variation of the mobility parameter (τ_c), evaluated from the EPR spectra at 298 K, for the various probes used in the present study, in the absence and in the presence of 4.5-SBD. The intermediate generation value ($G = 4.5$) was chosen as representative for investigating the behavior of CAT*n*−SBD solutions. To permit the comparison of the mobility parameters, the concentrations of both the radicals (0.16 mM) and the 4.5-SBD were the same for all samples. To avoid cooperative binding at the water/SBD interface and to minimize the perturbation effect of the probe, the ratio of concentration was fixed at [4.5-SBD]/[CAT*n*] = 100 (SBD concentration as dendrimers, *not* head group concentration). In order to underline the effect of the hydrophobic chain, τ_c is plotted as a function of CAT chain length. In the absence of SBD, the increase in chain length causes a small decrease of mobility which is expected since the rotation of the nitroxide group is increasingly hindered as the attached chain grows in length. This effect is strongly enhanced when 4.5-SBD is present. The mobility of CAT*n* decreases almost linearly with increasing n, up to $n = 12$. However, the τ_c evaluated for CAT16 in 4.5-SBD solution was almost the same as for CAT12. Since the positively charged group is always the same and common to all of the probes, the quenching in mobility can only be ascribed to the presence of the hydrophobic chain.

The aggregation of the carbon chains, which might occur to minimize the repulsions between the hydrophobic chain and polar groups, could induce an increase of τ_c. This possibly may

(26) Fox, K. K. *Trans. Faraday Soc.* **1971**, *67*, 2802.

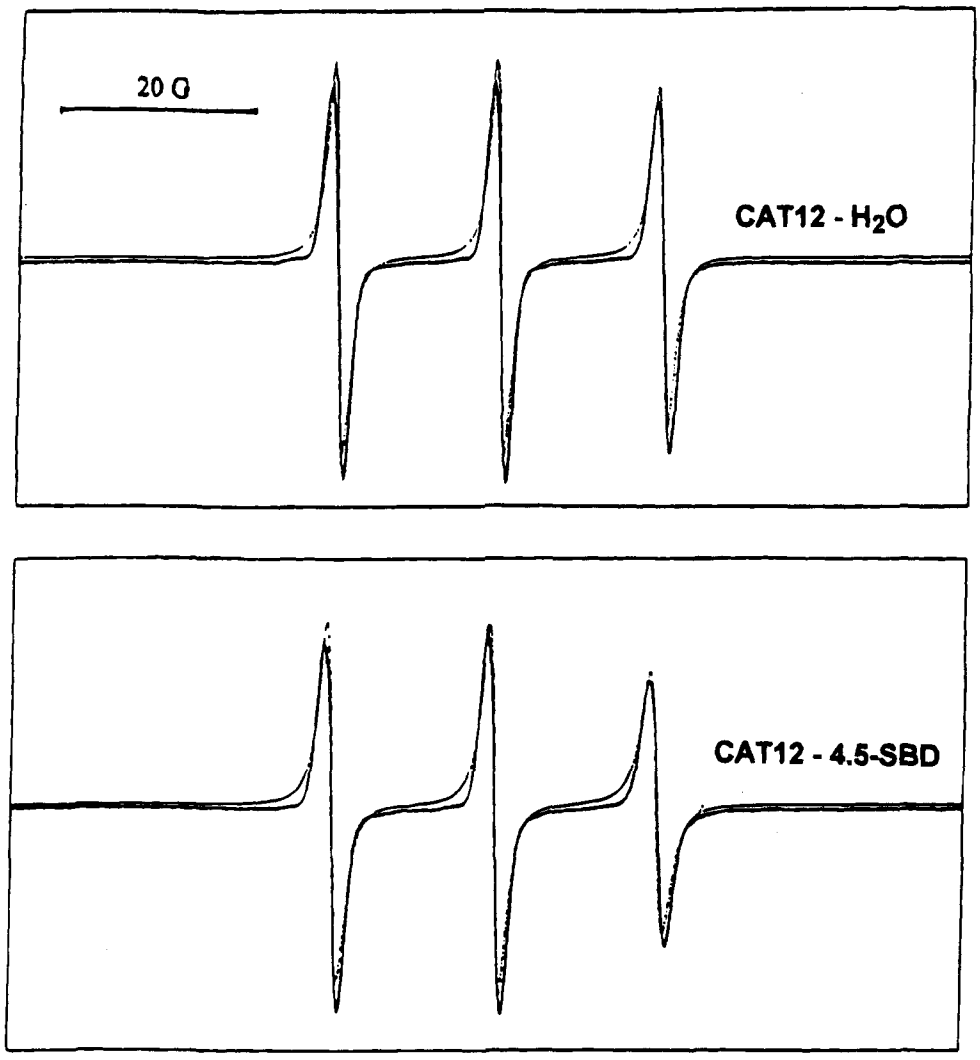

Figure 2. Experimental (full lines) and computed (dashed lines) EPR spectra of CAT12 (0.16 mM) in water solution and in solution containing 4.5-SBD at [SBD-COO^-] = 0.76 M.

be ruled out, since the radicals were highly diluted in solution. Only CAT16 may partially aggregate at these concentrations (if the cmc is lowered by the presence of *n*.5-SBDs).[27] Furthermore, the aggregation of probes should give rise to spin–spin interactions among the nitroxide groups, and the corresponding spectrum is an exchanged narrowed single line. The spectra analyzed in the present study are always the three narrow-line signals originated from monomeric nitroxide radicals at significant distances from each other.

The hydrophobic chains may interact with hydrophobic sites in the internal SBD structure, and this immediately explains the increase in τ_c with the increase in chain length. Other experimental results in this paper (see below) also support the conclusion that the probes anchor their chain at internal sites into the *n*.5-SBD structure. Furthermore, similar results have been observed for cationic surfactants interacting with polyanions.[28]

Therefore, we hypothesize that the carbon chain of the surfactant probes may partially penetrate the internal SBD structure to interact with sites of low polarity (very probably the $-COCH_2CH_2N=$ moieties). Deeper penetration and/or stronger hydrophobic interaction are expected with the increase in chain length. Kwak and co-workers[28,29] have estimated the free energy (ΔG, in units of kT) of binding with polyanions per CH_2 group of cationic surfactants. The value of ΔG ranges between 1.10 and 1.32 kT for various surfactants and polyanions, and is comparable to the free energy of micellization of the surfactants. This means that there is a competition for surfactant self-aggregation and binding to the polyanion. As discussed above, the very low concentration of the surfactants leads to negligible self-aggregation. Therefore, a marked predomination of the interaction with the hydrophobic SBD sites is expected and is consistent with the results.

2. pH Variations. Figure 4 shows the variation of the mobility parameter (τ_c) as a function of pH for CAT12 (0.3 mM) in 3.5-SBD and 7.5-SBD at a concentration of 0.32 M (parameters evaluated from EPR spectra at 293 K). The 3.5- and 7.5-SBDs were chosen as representative of the behavior of earlier and later generations, respectively. Furthermore, CAT12 was chosen since, as described in the previous paragraph (Figure 3), its mobility is largely dependent on the presence of the carbon chain. Therefore, CAT12 permits the study of the competition between hydrophobic and hydrophilic interactions between *n*.5-SBDs and the probe as a function of pH. The pH was varied in the range of 4–9, which ensures the stability of the radicals. In both 3.5-SBD and 7.5-SBD solutions the mobility of the probes is almost unaffected by the presence of

(27) Ottaviani, M. F.; Jockush, S.; Turro, N. J.; Tomalia, D. A. To be published.

(28) (a) Hayakawa, K.; Santerre, J. P.; Kwak, J. C. T. *Macromolecules* **1983**, *16*, 1642. (b) Hayakawa, K.; Santerre, J. P.; Kwak, J. C. T. *Biophys. Chem.* **1983**, *17*, 175.

(29) (a) Malovikova, A.; Hayakawa, K.; Kwak, J. C. T. *ACS Symp. Ser.* **1984**, *253*, 225. (b) Malovikova, A.; Hayakawa, K.; Kwak, J. C. T. *J. Phys. Chem.* **1984**, *88*, 1930.

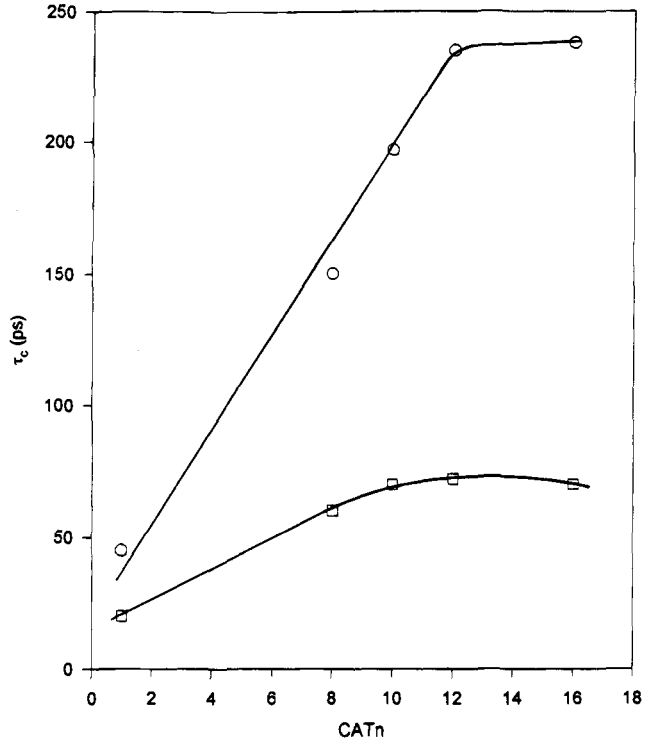

Figure 3. Variation of τ_c (ps), evaluated from the EPR spectra at 298 K, as a function of the radical chain length (indicated as CAT*n*; [CAT*n*] = 0.16 mM) in (□) water solution and in (○) solution containing 4.5-SBD ([SBD-COO$^-$] = 0.76 M).

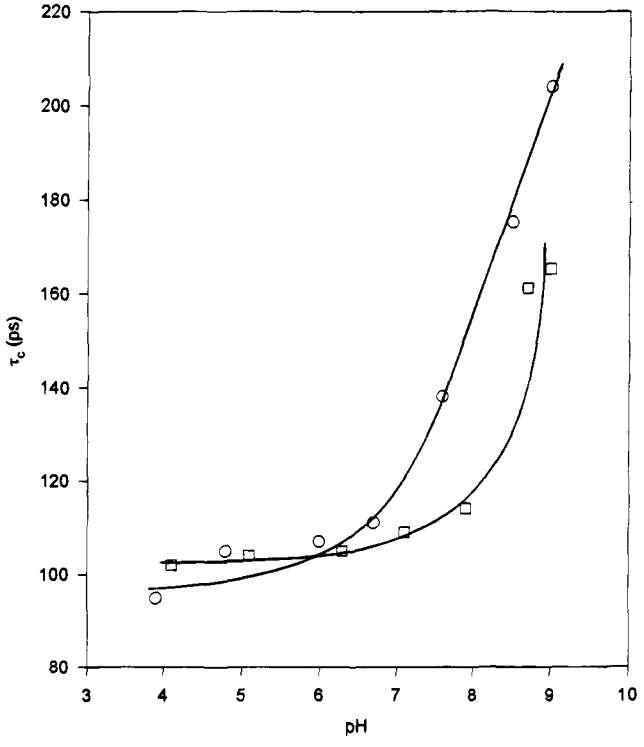

Figure 4. Variation of τ_c (ps), evaluated from the EPR spectra at 293 K, as a function of pH for CAT12 (0.3 mM) solutions containing (□) 3.5-SBD and (○) 7.5-SBD ([SBD-COO$^-$] = 0.32 M).

n.5-SBDs at pH < 6.5. However, as the pH was increased above 7.5, the correlation time for motion of 7.5-SBD solutions began increasing, whereas the 3.5-SBD solutions showed an increase of τ_c at pH ≥ 8. The effect is strongly indicative of a primary role of electrostatic interactions between the probe and the external SBD surface. The surface of the *n*.5-SBDs should remain negatively charged down to a pH as low as 3–4, due to ionization of the carboxylic groups. The carboxylic acid groups start deprotonating as the pH increases. Simultaneously the apparent pK_a is progressively shifted toward larger values by charge–charge repulsion. Therefore, electrostatic binding between the radicals and the deprotonated carboxylic groups may take place at pH > 6.5.

The interactions of CAT12 are stronger with the 7.5-SBD surface than with the 3.5-SBD one, due to the higher charge density of 7.5-SBD, i.e., a smaller distance between adjacent SBD-COO$^-$ groups (Table 1). In turn, the hydrophobic interactions, described in the previous section, may take place only when the electrostatic attractions are sufficient to allow approach of the positively charged radicals to the negatively charged *n*.5-SBD surface. The interactions between polyelectrolytes and oppositely charged surfactants have been previously described in terms of electrostatic attraction between opposite charges.[30–32] Therefore, the results discussed above indicate the simultaneous and cooperative effect of both hydrophilic and hydrophobic interactions.

The variation of polarity ($\langle A_N \rangle$) as a function of pH is rather small: 7.5-SBD samples show a decrease of $\langle A_N \rangle$ from 16.74_5 to 16.70 G for a variation of pH from 4 to 9. In the same range of pH, $\langle A_N \rangle$ changes from 16.75 to 16.71_5 G for 3.5-SBD samples. Indeed, even if the radical groups are affected by the surface charge and localize at the SBD–water interface, they are still localized in the water layers hydrating the SBD surface and the polarity at the surface itself is almost the same as in the bulk radical solution.

Analogous experiments in less polar media (acetonitrile–water) are in progress to better analyze the electrostatic attractions between the *n*.5-SBD surface at various levels of protonation and positively charged radicals.

3. Variations of SBD Generation at Constant [SBD–COO$^-$]. Figure 5 shows the plot of τ_c versus SBD generation for CAT1, CAT8, CAT12, and CAT16 at a constant ratio of [SBD-COO$^-$]/[CAT*n*] = 2000 (data calculated from the EPR spectra at 298 K). The general trend is a decrease of mobility with the increase in generation.

First of all, it is noteworthy that CAT1 shows a very small variation of mobility in the presence of *n*.5-SBDs of any generation, with respect to pure water. The latter is represented by a point $G = 0$ in Figure 5. Also the variation of $\langle A_N \rangle$ for CAT1 solutions is negligible with the increase in generation. On the basis of the similarities reported for *n*.5-SBDs with anionic micelles,[1a,c,i,10] we expected a rather significant variation of both mobility and polarity for CAT1 in the presence of the micellar-like macromolecules with respect to bulk CAT1 solutions. It has already been observed for CAT1 in sodium octyl, dodecyl, and hexadecyl sulfate (SOS, SDS, and SHS, respectively) solutions that both the mobility of the radical and its environmental polarity markedly decrease in correspondence with the critical micellar concentration of the surfactants.[16a] This behavior is related to the localization of CAT1 near the micellar surface, with partial binding to the hydrophobic micellar core. The main difference between micellar solution and *n*.5-SBD solutions resides in the fact that the micellar core is mainly hydrophobic, whereas the *n*.5-SBD internal structure is mainly hydrophilic. Therefore, the radical may penetrate the micellar surface in order to be stabilized by both hydrophobic and electrostatic interactions. An important result is the reported decrease in environmental polarity of CAT1 in micellar solu-

(30) Goddard, E. D. *Colloids Surf.* **1986**, *19*, 255, 301.
(31) Robb, I. D. In *Anionic Surfactants: Physical Chemistry of Surfactant Actions*; Lucassen-Reynders, E. H., Ed.; Marcel Dekker: New York, 1981; p 109.
(32) Goddard, E. D.; Hannan, K. B. In *Micellization, Solubilization and Microemulsions*; Mittal, K. L., Ed.; Plenum Press: New York, 1977; Vol. 2.

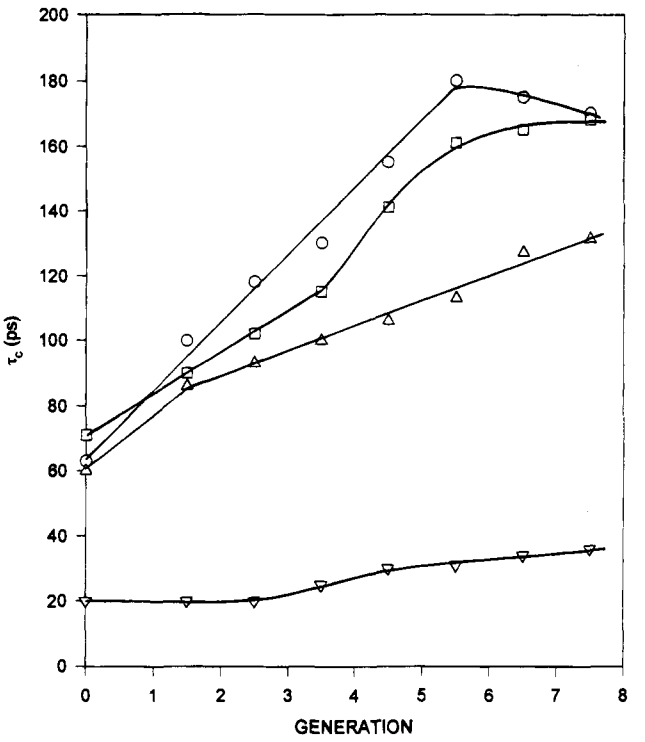

Figure 5. Variation of τ_c (ps), evaluated from the EPR spectra at 298 K, as a function of generation for solutions of *n*.5-SBD ([SBD-COO$^-$] = 0.32 M) containing (▽) CAT1, (△) CAT8, (□) CAT12, and (○) CAT16 ([CAT*n*] = 0.16 mM).

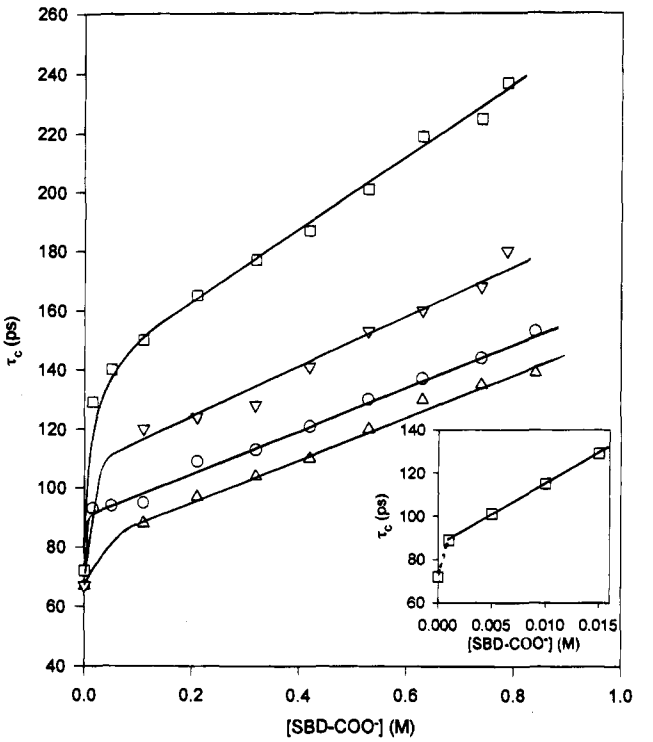

Figure 6. Variation of τ_c (ps), evaluated from the EPR spectra at 298 K, as a function of [SBD-COO$^-$] for solutions of 3.5-SBD and 6.5-SBD containing CAT8 and CAT12 ([CAT*n*] = 0.16 mM): (□) 5.5-SBD−CAT12, (▽) 5.5-SBD−CAT8, (○) 2.5-SBD−CAT12, (△) 2.5-SBD−CAT8. The inset in the figure reports in detail the plot of τ_c, evaluated from the EPR spectra at 298 K, for the lowest 6.5-SBD-COO$^-$ concentrations.

tions, together with the increase in the correlation times for motion.[16a] In contrast, CAT1 in *n*.5-SBD solutions is mainly localized in the hydration layers of the SBD surface and probably undergoes fast exchange between the bulk solution and the surface.

A core more hydrophobic than the internal structure of *n*.5-SBDs, such as the core of the dendritic macromolecules described in refs 5−9, is expected to be more interactive with the carbon chain of the radicals. A study on this subject is in progress.

To analyze the results from systems CAT8, CAT12, and CAT16 in the presence of *n*.5-SBDs (Figure 5), we must keep in mind that the EPR spectra for the various generations of SBDs were performed at constant SBD-COO$^-$ concentration. Therefore, the variation of the parameters cannot be ascribed to variations in electrostatic interactions between the SBD-COO$^-$ groups and the CAT moiety. However, the following effects should be considered: (a) Modifications of surface charge density with generation (Table 1). This seems to operate in the opposite direction with respect to the trend shown in the graph in Figure 5: as reported in Table 1, the averaged distance among the COO$^-$ surface groups is almost constant up to generation 5.5, and quickly decreases at higher generations. Therefore, the decrease of mobility and polarity up to generation 5.5 cannot be ascribed to the charge density variations. On the contrary, the higher charge density at higher generations may explain the inversion of slope for CAT16 and the almost constant parameters for CAT12: the more hydrophobic the probe, the lower the affinity toward the densely packed charged groups at the higher generations. (b) The availability of internal hydrophilic and hydrophobic interacting sites increases with the increase in size of the dendrimers; i.e., the internal structure of SBD offers increasing possibilities of interaction with the increase of generation. As described above, also partially hydrophobic groups are available and their number increases with the increase in generation. Furthermore, the hydrophobicity of the shell of *n*.5-SBDs just beyond the surface increases as the generation increases, due to the increasing density of the organic groups (Figure 1). Therefore, the presence of the carbon chain attached to the nitroxides, which may enter the SBD structure, allows the enhanced slowing of the probes' motion by increasing both generation and carbon chain length.

Hydrophobic interactions also account for a small decrease in environmental polarity, i.e., by increasing the generation, $\langle A_N \rangle$ decreases from 16.75 to 16.72 for CAT8, from 16.76 to 16.71$_5$ for CAT12, and from 16.82 to 16.76 for CAT16. Therefore, CAT16 shows the largest variation in $\langle A_N \rangle$ with the increase in generation, but the environmental polarity is higher with respect to shorter chain nitroxides at any generation. These results may be interpreted as follows: (1) Hydrophobic interactions between the carbon chain and the SBD internal structure may only partially perturb the polar environment of NO (small variations of $\langle A_N \rangle$), since the nitroxide group is localized in the water layers hydrating the SBD surface. (2) The longer the hydrophobic chain of CAT*n*, the better the penetration into the internal *n*.5-SBD structure, and the probe is affected to a greater extent by the increase in available hydrophobic sites with the increase in generation. As a consequence the variations of both mobility and polarity are larger as the chain grows longer and is more hydrophobic.

4. Increase in Concentration of SBD-COO$^-$. Figure 6 gives the plot of τ_c (evaluated from the EPR spectra at 298 K) vs the SBD-COO$^-$ concentration for CAT8 and CAT12 (0.16 mM) in the presence of 3.5-SBD and 6.5-SBD. These samples have been chosen as representative in order to analyze the effect of [SBD-COO$^-$] variations on earlier (3.5-SBD) and later (6.5-SBD) generations and the effect of [SBD-COO$^-$] variations on shorter (CAT8) and longer (CAT12) carbon chains of nitroxides. The main consequence of increasing the SBD-COO$^-$ concentration is the decrease in mobility, which is almost linear at rather large carboxylate concentrations ([SBD-COO$^-$] > 0.1 M). The

radicals are under fast motion conditions ($\tau_c < 1-3 \times 10^{-9}$ s) in the entire range of SBD-COO$^-$ concentrations, and the EPR spectra always consist of a single contribution (no superimposed signals are recognizable in the EPR pattern). These facts further support the conclusion that nitroxide groups are rather free to move in the solution layers at the SBD/water interface. Fast exchange of the radicals among different SBD hydration water layers is also consistent with the results. In the latter case the measured correlation time for motion is the averaged value among the various localizations. However, since the hydrophobic carbon chain partially enters the internal SBD structure, the probability for a fast exchange mobility of the nitroxide group in the external water layers is rather low. Indeed, the increase of SBD-COO$^-$ interacting sites also coincides with the increase of availability in internal interacting sites, which may give an anchorage point to the radical by means of its carbon chain. On the other hand, the positively charged groups of the radicals are expected to be mainly involved in electrostatic binding with the carboxylate groups at [SBD-COO$^-$]/[CAT*n*] > 500. Furthermore, the increase in SBD-COO$^-$ concentration at [SBD-COO$^-$] > 0.1 M does not increase the local charge density, since, for the same *n*.5-SBD, the increase in SBD-COO$^-$ corresponds to the increase in concentration of macromolecules and the carboxylate–carboxylate average distance is mantained. Nevertheless, the increased concentration of macromolecules increases the ionic strength in solution and could affect the mobility of the radicals. In this respect, it is noteworthy that $\langle A_N \rangle$ slightly decreases with the increase in [SBD-COO$^-$]: at [SBD-COO$^-$] > 0.1 M, $\Delta(\langle A_N \rangle)$ is about 0.03 G for the four samples tested in Figure 6. An increase in ionic strength leads to an increase in environmental polarity, whereas the opposite result is found in our systems. In conclusion, the linear growth of τ_c with SBD-COO$^-$ concentration is probably due to the increase of internal sites in the *n*.5-SBD structure.

From Figure 6 it is clearly seen that the variations of mobility with [SBD-COO$^-$] are different in both their relative values and the slope of the lines for the four representative samples. The trend in mobility is as follows: CAT8 in 3.5-SBD > CAT12 in 3.5-SBD > CAT8 in 6.5-SBD > CAT12 in 6.5-SBD. Therefore, 6.5-SBD is more effective in decreasing the radical mobility with respect to 3.5-SBD, as described above, but this persists in the entire range of SBD-COO$^-$ concentrations investigated. The same holds for CAT12 with respect to CAT8. This last finding is again connected to the occurrence of hydrophobic interactions between the carbon chain and the internal partially hydrophobic sites of SBDs, whose number increases with the increase of [SBD-COO$^-$]. The larger slope for CAT12 in 6.5-SBD therefore indicates a larger availability of internal interacting sites for the carbon chain.

The inset in Figure 6 shows the variation of τ_c for CAT12 in 6.5-SBD for the lowest SBD-COO$^-$ concentrations ([SBD-COO$^-$] ≤ 0.015 M). In the range 1 < [SBD-COO$^-$]/[CAT12] < 100–200 the variation of τ_c is again linear with the increase in [SBD-COO$^-$], but the slope is much higher (about 20 times) with respect to larger carboxylate concentrations. This larger linear growth of τ_c with [SBD-COO$^-$] is defined between two boundaries: the first one (low limit) corresponds to one CAT12 molecule for each SBD-COO$^-$ group (indeed, for [SBD-COO$^-$]/[CAT*n*] ≤ 1 precipitation occurs, due to neutralization of the SBD charge); the second boundary (high limit) roughly corresponds to one CAT12 molecule for each 6.5-SBD macromolecule. Therefore, the first larger increase in τ_c with [SBD-COO$^-$] in the range 0.16 mM ≤ [SBD-COO$^-$] ≤ 0.015 M is due to radicals which bind to interacting sites in the same macromolecule. The second smaller slope—corresponding to the variation of τ_c vs [SBD-COO$^-$] at [SBD-COO$^-$] > 0.1 M—coincides with the binding of nitroxide molecules with interacting sites belonging to different SBD macromolecules.

Table 2. τ_C/τ_B for CAT12 and CAT8 in solutions of 3.5- and 6.5-SBDs ([SBD-COO$^-$] = 0.11 and 0.63 M)

CAT	SBD	[SBD-COO−] (M)	τ_C/τ_B
12	3.5	0.63	1.43
12	3.5	0.11	1.30
12	6.5	0.63	1.17
12	6.5	0.11	1.12
8	3.5	0.63	1.17
8	3.5	0.11	1.14
8	6.5	0.63	1.09
8	6.5	0.11	1.07

It is noteworthy that, even at the lower [SBD-COO$^-$]/[CAT*n*] ratios, no evidence of spin–spin interactions, expected for CAT*n* molecules in close vicinity, is found from EPR spectral analysis. The concentration of radical molecules in solution is indeed very low, and no cooperative binding is expected under such conditions.

It is of interest to analyze the anisotropy of motion which is simply evaluated as τ_C/τ_B (for the definition of τ_C and τ_B see the section on the evaluation of mobility and polarity parameters). The τ_C/τ_B values are reported in Table 2 for the samples used for Figure 6 at two different SBD-COO$^-$ concentrations (0.63 and 0.11 M).

The main findings are (i) higher anisotropy for 3.5-SBD with respect to 6.5-SBD, (ii) higher anisotropy for CAT12 with respect to CAT8, and (iii) higher anisotropy at higher concentrations of SBD-COO$^-$.

The larger anisotropy for 3.5-SBD may be related to the morphology of early generation SBDs: the open structure forces the radical to rotate faster in the "parallel" direction (usually corresponding to the direction of the p_z orbital on the nitrogen atom containing the unpaired electron) with respect to the "perpendicular" direction (the N–O direction). The increases in carboxylate concentration and in the radical chain length give a slight increase in anisotropy of motion due to the increase in availability of interacting sites and the gain in hydrophobic interactions, respectively.

5. Variation of Temperature. All the spectra discussed in the above sections were recorded at room temperature. The line shape variations with temperature are usually very informative on the type and mechanism of interaction of paramagnetic species on surfaces.[33] Figure 7 shows the variation of τ_c (on the logarithmic scale) as a function of *T* for CAT1 (0.16 mM) in 3.5-SBD (0.88 M) and 6.5-SBD (0.66 M) solutions. The range of temperature investigated was 100 K (between 230 and 330 K). All the values of correlation times for motion were evaluated by computation of the EPR spectra to obtain good compatibility among parameters evaluated in the different regions of mobility, that is, fast motion, $\tau_c < (1-3) \times 10^{-9}$ s, and slow motion, $(1-3) \times 10^{-9}$ s < τ_c < 5×10^{-7} s (rigid motion conditions—$\tau_c > 5 \times 10^{-7}$ s—were not experienced by these systems in the range of *T* investigated). The concentrations of SBD were 0.88 M for 3.5-SBD and 0.66 M for 6.5-SBD in order to have the same mobility conditions at the lower temperatures (*T* < 243 K).

The main features of the results are as follows: (a) At higher temperatures an almost linear plot of log τ_c versus *T* is obtained. From the variation of $-\log \tau_c$ as a function of $1/T$ the activation energy for rotational mobility was evaluated: $\Delta E^* = 4.4$ kcal/mol, which is smaller than for CAT1 in water solution (5.0 kcal/

(33) (a) Martini, G.; Ottaviani, M. F.; Romanelli, M *J. Colloid Interface Sci.* **1983**, *94*, 105. (b) Romanelli, M.; Ottaviani, M. F.; Martini, G. *J. Colloid Interface Sci.* **1983**, *96*, 373. (c) Martini, G.; Ottaviani, M. F.; Romanelli, M *J. Colloid Interface Sci.* **1987**, *115*, 87.

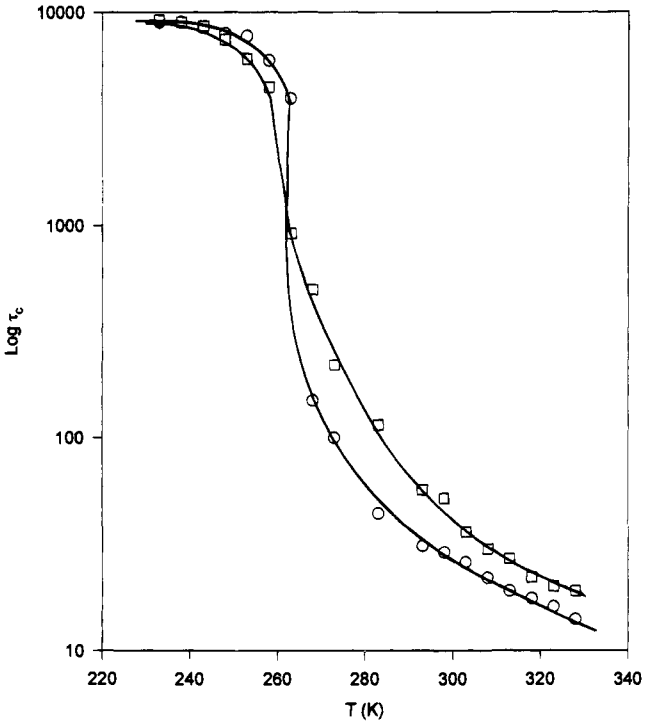

Figure 7. Variation of τ_c (ps), on the logarithmic scale, as a function of temperature (K) for solutions of (○) 3.5-SBD ([SBD-COO$^-$] = 0.88 M) and (□) 6.5-SBD ([SBD-COO$^-$] = 0.66 M) containing CAT1 (0.16 mM).

mol). (b) At higher temperatures, the mobility in 6.5-SBD solution is lower than the mobility in 3.5-SBD, in spite of the lower concentration of 6.5-SBD solution with respect to the concentration of the 3.5-SBD solution. (c) The spectra show a progressive decrease of the motion of the radicals over a large range of temperature; i.e., the solutions do not freeze at a given temperature, but exhibit a glass transition with the decrease of temperature. The *n*.5-SBDs modify the rheological properties of the surrounding water molecules. Nitroxides confined in microheterogeneous media have already shown such behavior.[33] (d) The glass transition is more gradual for 6.5-SBD solution with respect to 3.5-SBD solution. As a result CAT1 in 3.5-SBD solution presents lower mobility than CAT1 in 6.5-SBD solution, in the range 250−270 K. The above finding is related to the morphology of SBDs. The open structure of 3.5-SBD allows an easier equilibration for the water molecules exchanging between internal pools and the external solution, and the quenching is therefore faster for the radicals in 3.5-SBD than for CAT1 in 6.5-SBD solution. (e) At 240 K the mobility is almost the same as at 77 K for both 3.5-SBD and 6.5-SBD solutions.

As was already tested, CAT1 may undergo fast exchange within the water layers sorrounding the *n*.5-SBD surface. The modifications of the properties of water due to the SBD surface charge are probably rather far from the surface itself. This leads to a decrease in the mobility of the probe (forming a glass structure) at rather high temperature.

The long chain nitroxides provide evidence for a glass transition in *n*.5-SBDs solutions. Figure 8 shows the experimental EPR spectra of CAT12 solutions at concentrations of 0.3 and 1.6 mM in the presence of 3.5-SBD 0.89 M, at various temperatures. The 0.3 mM solution of CAT12 undergoes a progressive decrease in mobility. However, the radicals still show fast motion conditions at 263 K, and slow motion conditions were only found at 253 K. The spectra at various temperatures of the 1.6 mM solution of CAT12 show a largely different behavior with respect to the spectra from the more diluted solution. First of all, the motion of the radical is already slow at 263 K. With a decrease in temperature, the EPR spectra initially show the progressive resolution of the anisotropic components of the **g** and **A** tensors, as expected for a glass transition, and then a broad unresolved signal starts contributing to the overall EPR spectra. This signal remains almost the only contribution to the spectra at temperatures below 233 K. Such behavior at low temperatures is found whenever the radical surfactants aggregate in solution (results not shown). CAT12 has a cmc of 7.1 mM;[33] therefore, micelles of CAT12 are not expected at concentrations as low as 1.6 mM. The decrease of the cmc for CAT12 is therefore accounted for by the presence of 3.5-SBD in the solutions. It is noteworthy that, even if the spectra at room temperature do not detect the formation of surfactant aggregates in solution (i.e., an exchange-narrowed signal due to the formation of aggregates is not visible in the EPR spectra), the line shape variation as a function of temperature, shown in Figure 8b, is symptomatic of aggregate formation. On the other hand, the broad signal prevents the accurate measure of the spectral parameters.

Arrhenius linear plots were obtained for the long chain nitroxides in the range of temperature of 298−263 K, as shown in Figure 9. In detail, Figure 9a shows the Arrhenius plots for CAT12 (0.3 mM) in water and in 2.5-, 4.5-, 6.5-, and 7.5-SBDs (0.32 M). Figure 9b displays the plots for CAT12 at two different concentrations (0.3 and 1.7 mM) in 3.5-SBD solution at two different concentrations (0.36 and 0.89 M). Finally Figure 9c presents the plots for CAT8 (1.7 mM) in water and in 2.5-SBD solutions at two different concentrations (0.26 and 1.32 M). The results are discussed in terms of the correlation times for motion at 283 K and the activation energies for the rotational motion, which are reported in Table 3.

The main findings may be summarized as follows: (i) An increase in generation (constant [CAT*n*] and [*n*.5-SBD], the same radical) is accompained by a decrease in ΔE^* and an increase in τ_c (up to $G = 6.5$). (ii) An increase in [SBD-COO$^-$] (constant [CAT*n*] and generation, the same radical) results in an almost constant ΔE^*, but an increase in τ_c. (iii) An increase in [CAT*n*] (constant [SBD-COO$^-$] and generation, the same radical) results in an increase in ΔE^* and an increase in τ_c. (iv) An increase in radical chain length causes an increase in ΔE^* and an increase in τ_c.

The variations of the correlation times were already discussed in the above sections, whereas the variations of ΔE^* need further comment. First of all, a decrease in ΔE^* with respect to the value in water solution has already been described for nitroxide radicals in microheterogeneous systems.[33a,c] The restriction of degrees of freedom is due to trapping of the probe in a restricted space which exists in the proximity of the interacting surfaces. In the present case, the increase in generation gives the same effect, which is in line with the occurrence of stronger hydrophilic and hydrophobic interactions and trapping of the probe at the SBD/water interface.

The increase in ΔE^* with the increase in [CAT*n*] and the radical chain length can be explained by taking into account the aggregation of the surfactant molecules. This matter needs further analysis, and a study, by means of spin-probes and spin-labels, is in progress on the aggregation process of surfactants in the presence of *n*.5-SBDs.

Conclusions

Positively charged nitroxide radicals, possessing hydrocarbon chains of systematically varying lengths, have been shown to be very good probes to analyze the structure and the binding

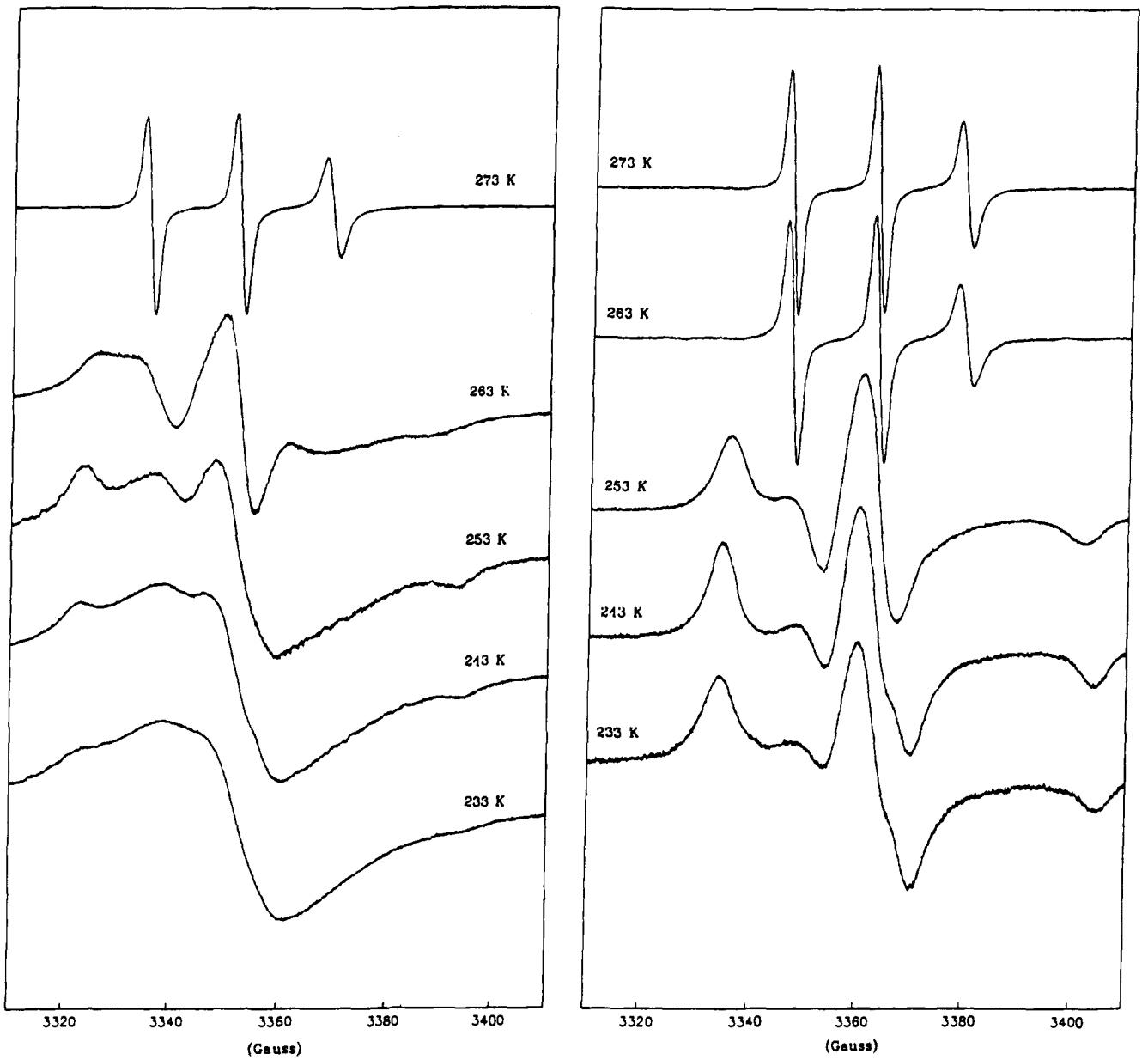

Figure 8. EPR experimental spectra of solutions of 3.5-SBD ([SBD-COO^-] = 0.89 M) containing CAT12 at concentrations of 1.6 mM (a, left) and 0.3mM (b, right) at different temperatures.

ability of half-generation PAMAM dendrimers from generation 1.5 generation 7.5.

A detailed analysis of the EPR spectra allowed the evaluation of mobility (τ_c) and polarity (A_N) parameters. The following main points were addressed.

(1) Localization of the radical probes. The radicals maintain fast motion conditions ($\tau_c < 1-3 \times 10^{-9}$ s) in a wide range of SBD-COO^- concentrations and the spectra are always constituted by a single component (no superposition of different components due to radicals in different environments). Therefore, nitroxide groups are supposed to localize mainly in the water layers at the *n*.5-SBD/solution interface. However, the water molecules, which surround the probes, are affected by the SBD negative surface charge, since the solutions do not freeze at a certain temperature, but show a glass transition over a large range of temperature.

A decrease in the activation energy for rotational motion was found with the increase in generation and in chain length: the radicals are trapped in a restricted space in proximity to the dendrimer surface.

The schematic picture in Figure 10 gives an indication of the proposed localization of the probes CAT1 and CATn at the *n*.5-SBD/water interface.

(2) Difference between anionic micelles and *n*.5-SBDs. The smallest probe, CAT1, undergoes a very small, almost negligible, variation of both mobility and polarity in the presence of *n*.5-SBDs of any generation. This result contrasts with the significant variations of both τ_c and A_N previously found in micellar solutions. The micellar surface is therefore much more interactive toward CAT1, probably because the hydrophobic core allows the radicals to slightly penetrate the micellar surface, whereas the dendrimer core is mainly hydrophilic in nature and the main interactions are electrostatic or hydrophilic, keeping the probe in the water layers.

The electron-transfer quenching of photoexcited $Ru(Phen)_3^{2+}$ by methylviologen has proven the similarity between *n*.5-SBDs and anionic micelles,[10] which seems in contrast to the above conclusions. However, $Ru(Phen)_3^{2+}$ is expected to interact stronger than CAT1 with the dendrimer surface, due to the

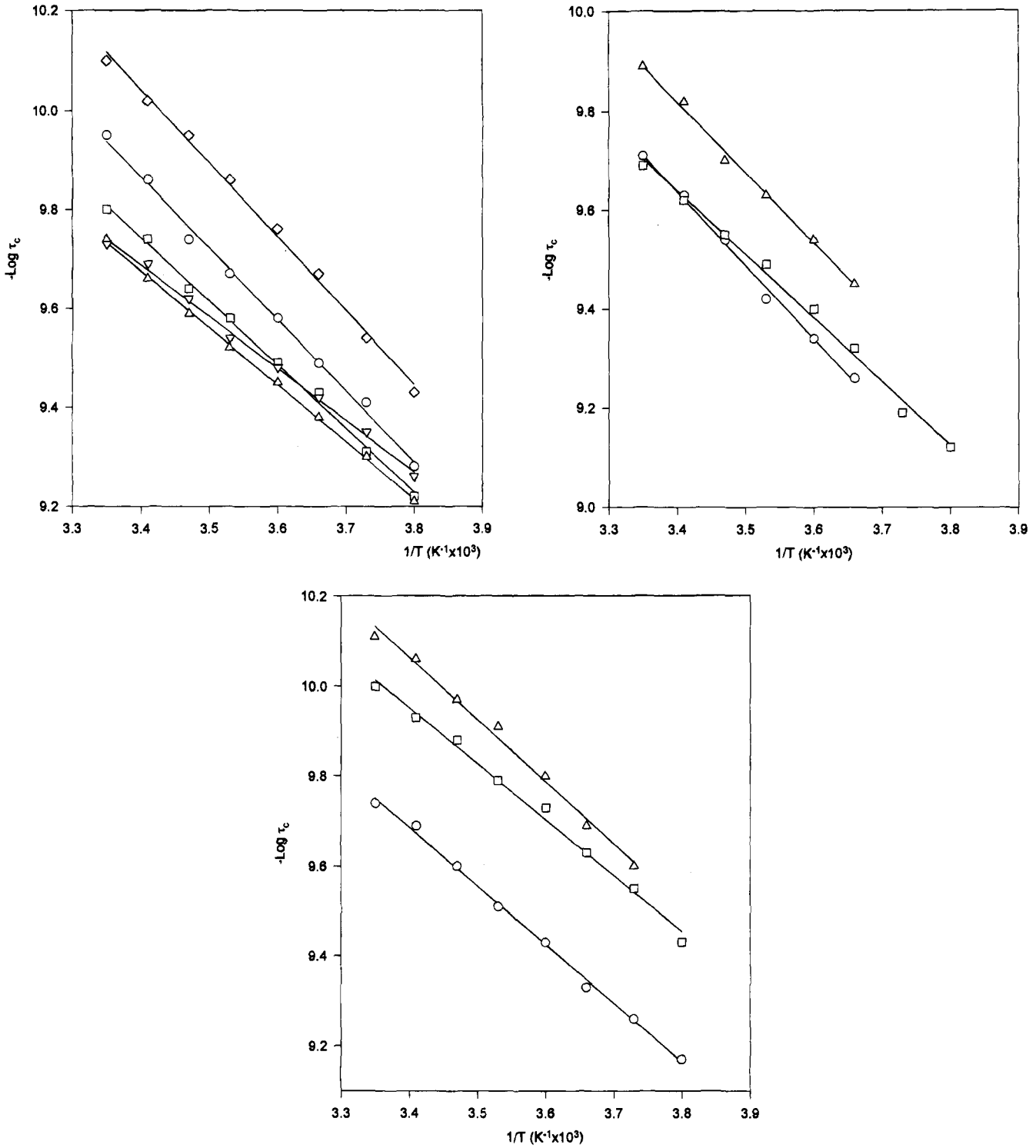

Figure 9. Arrhenius plots ($-\log \tau_c$ vs $1/T$) in the range of temperature 298-263 K for solutions of *n*.5-SBDs containing CAT12: (a, top left) (◇) water solutions and solutions of (○) 2.5-, (□) 4.5-, (△) 6.5-, and (▽) 7.5-SBDs ([SBD-COO^-] = 0.32 M) with [CAT12] = 0.3 mM; (b, top right) solutions of 3.5-SBD at [SBD-COO^-] = 0.89 M containing CAT12 at concentrations of (□) 0.3 and (○) 1.6 mM and (△) solutions of 3.5-SBD at [SBD-COO^-] = 0.32 M containing [CAT12] = 1.6 mM; (c, bottom) solutions of 2.5-SBD ([SBD-COO^-] = (○) 1.32 and (□) 0.26 M) containing CAT8 (1.7 mM) and (△) an Arrhenius plot of CAT8 in water (1.7 mM) shown for comparison.

presence of both a double positive charge and the planar phenanthroline group which may penetrate the internal SBD structure.

(3) Hydrophobic interactions between the carbon chain of the radicals and sites at low polarity in the internal SBD structure. The decrease in mobility with the increase in nitroxide chain length was ascribed to the presence of the hydrophobic chain binding to hydrophobic sites of the *n*.5-SBDs. We hypothesize that the carbon chain may penetrate the internal SBD structure to interact with sites of low polarity (very probably the $-COCH_2CH_2N=$ moieties). This proposal also explains the decrease in mobility with the increase in generation: the internal structure of the *n*.5-SBDs offers increasing possibilities of interaction with the increase of generation; i.e., the number of interacting sites of *n*.5-SBDs increases as the dendrimer size increases (this also holds true if the SBD-COO^- concentration is constant). Furthermore, the density of the organic groups just behind the SBD surface increases as the generation increases (see Figure 1): the hydrophobicity of the core layer adjacent to the SBD surface increases as the

Table 3. Correlation Times for Motion at 283 K and Activation Energies for the Rotation Diffusional Motion for CAT8 and CAT12 in Water and in Solutions of *n*.5-SBDs

CAT*n*	[CAT*n*] (mM)	*n*.5-SBD	[SBD-COO$^-$] (M)	τ_c(283 K) (10^{-10} s)	(kcal/mol)
CAT12	0.3	water		1.39	6.9
CAT12	0.3	2.5-SBD	0.32	2.11	6.6
CAT12	0.3	4.5-SBD	0.32	2.64	5.9
CAT12	0.3	6.5-SBD	0.32	2.98	5.3
CAT12	0.3	7.5-SBD	0.32	2.90	4.8
CAT12	0.3	3.5-SBD	0.89	3.26	5.8
CAT12	1.7	3.5-SBD	0.89	3.77	6.6
CAT12	1.7	3.5-SBD	0.32	2.32	6.6
CAT8	1.7	water		1.24	6.5
CAT8	1.7	2.5-SBD	0.26	1.61	5.7
CAT8	1.7	2.5-SBD	1.32	3.10	5.9

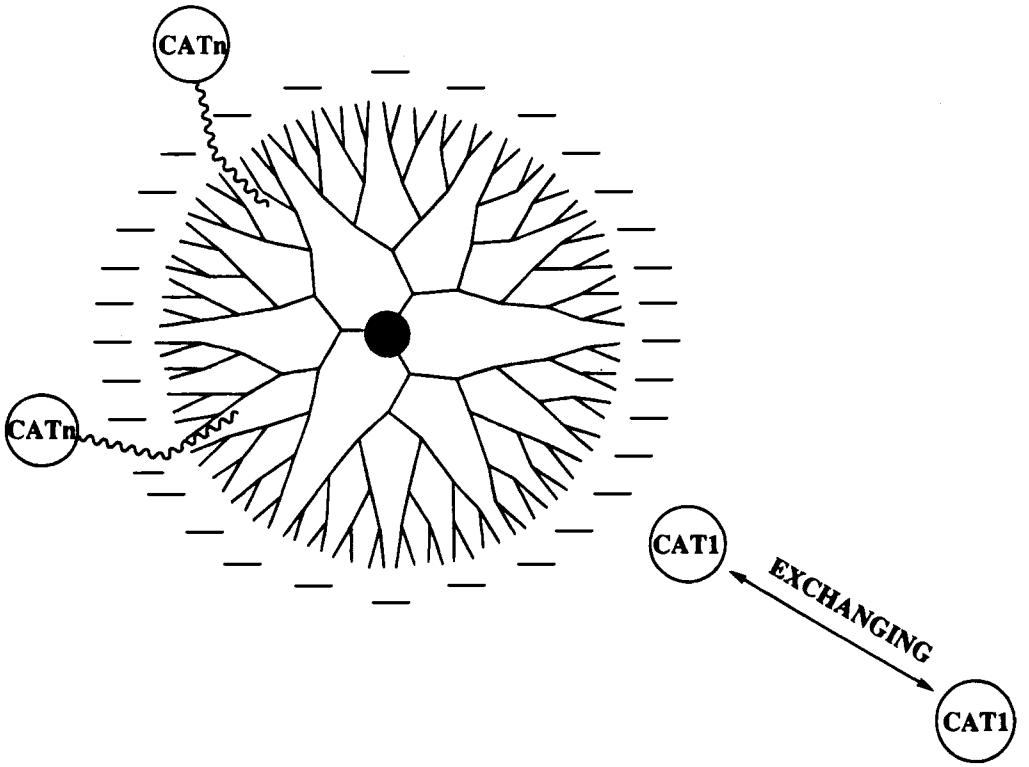

Figure 10. Scheme in a two-dimensional projection of the proposed localization of the CAT*n* radicals at the *n*.5-SBD/water interface.

dendrimer size increases, passing from earlier to later generations. Therefore, the hydrophobic interactions with the radical carbon chain are favored.

The linear relationship of τ_c and SBD-COO$^-$ concentration is also due to the correlated increase of internal sites in the *n*.5-SBD structure.

(4) Electrostatic interactions between the positively charged nitroxide radicals and the negatively charged SBD surface. The analysis as a function of pH reveals that electrostatic interactions between the probe and the external SBD surface are the driving forces to approach the positively charged radicals to the SBD-COO$^-$ groups. Only if the electrostatic interactions are sufficient do interactions with internal sites take place. The lower surface charge density of the earlier generation dendrimers is reflected by a weaker attractive effect with respect to later generations.

(5) Dendrimer morphology. All the results support the conclusions from molecular simulations[2] which indicates a change of the morphology of the starburst dendrimers from the earlier generations ($G < 4$) to the later generations ($G \geq 4$).

Acknowledgment. N.J.T. thanks the AFOSR and NSF for their generous support. D.A.T. thanks the New Energy and Development Organization (NEDO) of the Ministry of International Trade and Industry of Japan (MITI) for its generous support and certain critical synthetic efforts. M.F.O. and E.C. thank the Italian Ministero Università e Ricerca Scientifica e Tecnologica (MURST), the Italian Consiglio Nazionale delle Ricerche (CNR), and NATO for their financial support.

JA943929Q